2024-04-13

Experimental investigation of mechanical properties of GGBS-FA-SF blended geopolymer concrete at elevated temperatures

Wang, T

10.1016/j.firesaf.2024.104156
Fire Safety Journal
Elsevier BV

Experimental investigation of mechanical properties of GGBS-FA-SF blended geopolymer concrete at elevated temperatures

Tan Wang[a], Min Yu[a,b], Hanjie Lin[a], Dawang Li[b,c], Long-yuan Li[b*]

a) School of Civil Engineering, Wuhan University, Wuhan 430072, China

b) School of Engineering, Computing and Mathematics, University of Plymouth, Plymouth PL4 8AA, UK

c) Guangdong Provincial Key Laboratory of Durability for Marine Civil Engineering, Shenzhen University, Shenzhen 518060, China

* Corresponding author

Abstract – Geopolymer has excellent mechanical properties at elevated temperatures, but geopolymer concrete may not be so because of the large difference in thermal properties between geopolymer and aggregate which could lead to substantial thermal stresses when they are in a high temperature environment. In this paper we present an experimental investigation on the mechanical properties of GGBS-FA-SF blended geopolymer concrete with and without steel fibres at elevated temperatures. The influences of exposure temperature, coarse aggregate and steel fibre on the failure mode, compressive strength, elastic modulus, peak strain, and ductility of the geopolymer mortar and geopolymer concrete are examined. Based on the experimentally obtained data, empirical temperature-dependent stress-strain constitutive equations are also proposed, which can be used for the fire safety analysis and design of geopolymer concrete with and without steel fibres.

Keywords: Geopolymer concrete; Mechanical properties; Elevated temperature; Constitutive equation; Steel fibres; Fire

1. Introduction

The fire safety of building structures is an important issue in modern structural design. Successful fire safety design requires an understanding of the behaviours of structures and materials at elevated temperatures [1]. Concrete is the mostly used construction and building material. The structural fire safety capacity of concrete is very complicated because concrete is a heterogeneous material with considerable variations. When it is subjected to elevated temperatures such as a fire the concrete experiences not only physical but also chemical changes which lead to the deterioration of its material and mechanical properties [2]. Geopolymer concrete (GPC) is a new type of concrete which is made by reacting aluminate and silicate bearing materials such as fly ash (FA) and/or ground granulated blast-furnace slag (GGBS) with alkaline activators. Thus, the mechanical behaviour of GPC at elevated temperatures is significantly different from that of ordinary Portland cement concrete [3]. In addition, the development in GPC mix design by using different precursors has led to different GPC types which, besides having an increased structural performance at ambient temperature, have also shown a different performance when exposed to elevated temperatures [4].

The importance of understanding the behaviour of different GPC materials in fire is very certain. Great effort has been made in recent years to study the micro-material and macro-mechanical properties of GPC at various elevated temperatures [3,4]. For example, Abdulkareem et al. [5] presented a comparative study on the influence of elevated temperature on FA-based geopolymer paste, mortar and lightweight aggregate concrete. It was shown that, at ambient temperature the geopolymer paste and mortar have significantly high strength compared to the lightweight aggregate concrete, but not at elevated temperatures. Zhang et al. [6]

reported an experimental investigation on the mechanical properties and thermal behaviours of metakaolin-FA blended geopolymer mortar at ambient temperature and after exposure to elevated temperatures. It was found that the geopolymer mortar exhibited higher temperature-induced degradation in bending and tensile strengths, but lower degradation in compressive and bond strengths than ordinary Portland cement mortar. Su et al. [7] investigated experimentally the mechanical properties of GPC under dynamic compression at elevated temperatures. It was found that the dynamic compressive strength of GPC was higher at 200°C than at ambient temperature and had a dramatic drop at 800°C. Shaikh and Hosan [8] examined the effects of Na and K-based alkaline activators on the residual mechanical properties of steel fibre reinforced GPC after exposed to various elevated temperatures. It was shown that the steel fibre reinforced GPC containing Na-based activators exhibited much higher residual compressive and indirect tensile strengths at all elevated temperatures than that containing K-based activators. Jiang et al. [9] presented a comparative study on the effect of elevated temperature on FA-based geopolymer pastes. The study involves the thermo-physical behaviour, engineering performance, and microstructure of the geopolymers before and after the exposure. Jiang et al. [10] also presented an experimental study on the effect of elevated temperature on the thermal-physical behaviours and mechanical properties of FA-based geopolymer paste. Zhang et al. [11] reported the experimental results obtained from high temperature spalling tests on GPC. It was shown that the GPC exhibited better spalling resistance than ordinary Portland cement concrete, and its permeability experienced a significant evolution with exposure temperature especially above 500°C due to the sintering reaction in geopolymer binders at high temperature. Tayeh et al. [12] examined the effect of high temperature on both lightweight GPC and lightweight ordinary cement concrete. It was found that the lightweight GPC performed better in terms of the compressive strength. Dhasindrakrishna et al. [13] examined the effects of poly vinyl alcohol fibre on the rheology and fire resistance of geopolymer foam concrete. It was shown that the addition of fibre improved the compressive strength by up to 54%. The residual compressive strength after exposure to elevated temperatures up to 200° was improved with the fibre until 2% dosage. However, further increase of fibre dosage deteriorated the residual strength. Salih et al. [14] examined the effect of elevated temperature on the microstructural properties of alkali-activated mortar blended with palm oil fuel ash and GGBS by using material characterisation test methods. Albidah et al. [15] investigated the behaviour of metakaolin-based GPC under ambient and elevated temperatures. The study used five mixes with different formulations to primarily investigate the influence of varying Na_2O/Al_2O_3 and SiO_2/Al_2O_3 molar ratios. It was found that the residual compressive strength varied from 56% to 63%, 38% to 51% and 28% to 34% after exposure to temperatures 200°C, 400°C, and 600°C, respectively. Trindade et al. [16] also examined the elevated temperature effect on the residual and quasi in-situ flexural strength of strain-hardening geopolymer composites reinforced with polyvinyl alcohol and ultra-high molecular weight polyethylene fibres. Zheng et al. [17] reported an experimental investigation of the mechanical properties of ultrahigh performance GPC against sulphate attack at elevated temperatures. It was shown that the ultrahigh performance GPC with lower CaO, higher Al_2O_3, and higher Si/Al exhibited superior sulphate corrosion resistance but deteriorated mechanical properties at elevated temperatures. Tahwia et al. [18] also examined the effect of high temperature up to 800°C on the compressive strength and microstructure of ultrahigh performance GPC. Özbayrak et al. [19] provided an experimental study on the effect of activator ratio on the mechanical properties of GPC at elevated temperatures. It was found that the ambient-temperature compressive strength increased but the elevated-temperature compressive strength decreased with the increased AA/FA ratio. Liu et al. [20] investigated the dynamic behaviour of high-performance GPC reinforced with steel fibres after

heating–cooling treatment by using P-wave velocity and quasi-static uniaxial compressive tests. It was found that the high-performance GPC reinforced with steel fibres suffered different degrees of thermal damage under temperatures 250–1000°C although it has good explosive spalling resistance. Zhang et al. [21] presented a comparison study of the performance of GPC and ordinary Portland cement concrete with and without fibres after exposure to temperatures 200, 500, and 800˚C. Yu et al. [22] presented an experimental and numerical investigation on the thermal properties of alkali-activated concrete at elevated temperatures. The work demonstrated that the thermal and mechanical properties of GPC when exposed to elevated temperatures are normally temperature dependent.

The above literature survey shows that, although there have been numerous studies on GPC at elevated temperatures, most of works focused only on the effect of elevated temperature on the compressive and tensile strengths of GPC blended with a single precursor, for instance, FA, GGBS, or metakaolin. There are very few works on the GPC blended with multiple precursors; and particularly there is a lack of study on the temperature-dependent stress-strain constitutive relation of GPC when exposed to elevated temperatures. In this paper, we present an experimental study on the mechanical properties of GPC, blended by using GGBS, FA and salic fume (SF) as the combined precursors, when exposed to various elevated temperatures. The GPC specimens tested include the geopolymer mortar and concrete, both with and without steel fibres. The experimental results obtained involve the failure mode, compressive strength, elastic modulus, peak strain, and stress-strain relation of GPC specimens when they were exposed to various elevated temperatures. Finally, based on the experimental data obtained, empirical temperature-dependent stress-strain constitutive equations are proposed which can be used for the fire safety analysis and design of geopolymer concrete with and without steel fibres.

2. Materials and experiments

2.1 Raw materials and mix designs

The raw materials used in the present experimental study include three precursors (GGBS, class F FA, and SF), two alkaline activators (sodium hydroxide (95% NaOH) with density of 2130 kg/m^3 and sodium silicate (30% SiO_2 and 13.5% Na_2O) with density of 1510 kg/m^3), fine aggregate (river sand of fineness modulus of 2.7), coarse aggregate (crushed stone of sizes ranging from 2 mm to 10 mm), and steel fibres (12 mm length straight steel fibres with aspect ratio of 45 and nominal tensile strength of ~2750 MPa). The mass ratio of GGBS/FA/SF used in the binder is 3.5/2.0/1.0 in all mixes. Table 1 gives the chemical and physical properties of the three precursors employed and corresponding mixed binder, and Fig. 1 shows the images of GGBS, FA, and SF obtained from scanning electron microscope (SEM). Table 2 gives the details of the mix designs used for making the specimens for experimental tests. Note that all the raw materials used and the mix designs adopted in the present experimental study are the same as those used in our previous works [22,23]. The four mix designs are labelled as S0CA0, S2CA0, S0CA30, and S2CA30, respectively, representing the geopolymer mortar (GPM) with no steel fibre (S0CA0), the steel fibre reinforced GPM with 2% steel fibre volume fraction (S2CA0), the GPC with 30% coarse aggregate volume fraction but no steel fibre (S0CA30), and the steel fibre reinforced GPC with 2% steel fibre volume fraction and 30% coarse aggregate volume fraction (S2CA30), respectively. The volume ratios of steel fibre and coarse aggregate were calculated based on their densities and mass ratios used in the mixes.

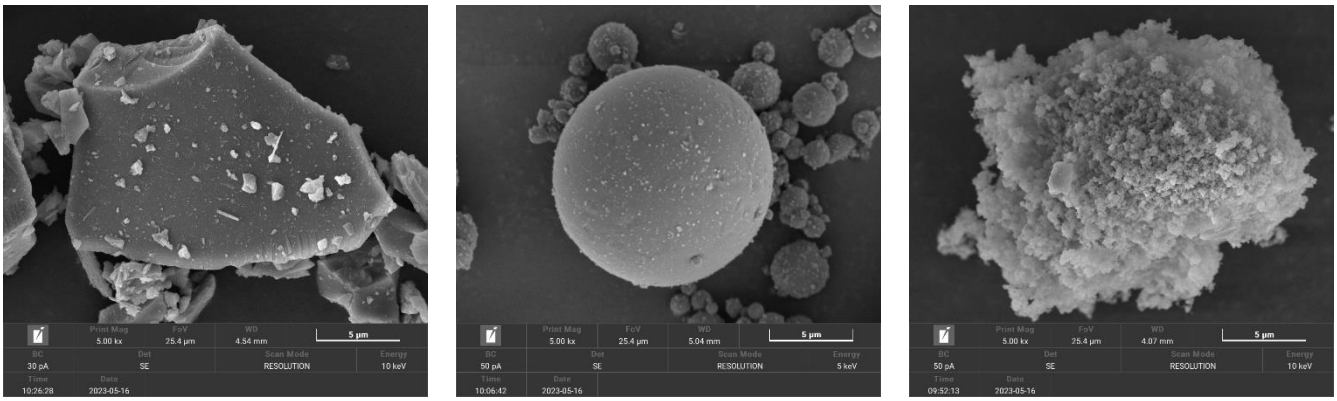

(a) GGBS (b) FA (c) SF

Fig. 1 SEM images (×5000) of GGBS, FA and SF

Table 1 Chemical and physical properties of raw materials

Composition	FA (wt.%)	GGBS (wt.%)	SF (wt.%)	Binder
SiO_2	51.8	35.5	95.8	49.8
Al_2O_3	29.7	13.3	0.48	16.4
Fe_2O_3	5.03	1.20	1.47	2.42
MgO	1.05	8.60	0.48	5.03
CaO	6.70	39.5	0.32	23.4
K_2O	2.42	0.25	0.73	0.991
Na_2O	0.54	0.55	0.41	0.525
SO_3	0.90	0.20	0.21	0.417
TiO_2	1.22	0.84	–	-
Others	0.64	0.06	0.09	0.243
Specific surface area (m^2/kg)	450	521	23200	-
Specific gravity (kg/m^3)	2390	2910	2200	-

Table 2 Mixes of GPM and GPC with and without steel fibres (units: kg/m^3)

Mix No.	GGBS	FA	SF	Fine aggregate	Water	Sodium silicate	NaOH	Steel fibre	Coarse aggregate
S0CA0	703	201	100	1105	229	254	6.77	\	\
S2CA0	689	197	98	1083	224	249	6.63	157	\
S0CA30	492	141	70	774	160	178	4.74	\	900

S2CA30	483	138	69	758	157	174	4.64	109.9	900

2.2 Preparation of specimens

The following procedures were used for the preparation of GPM and GPC specimens with and without steel fibres:

(1) Dry mixing: GGBS, FA, SF, fine aggregate, and coarse aggregate (for GPC specimens) were mixed using a hand-held mixer for two minutes. Afterwards, steel fibres were added into the mixer for the steel fibre reinforced GPM and GPC specimens for having another three minutes of dry mixing.

(2) Alkaline activator preparation: Sodium hydroxide was first dissolved in water and stirred for five minutes. Then sodium silicate was added into the solution and mixed for another five minutes to obtain the alkaline activator solution.

(3) Wet mixing: The alkaline activator prepared in step 2 was added into the mixer with dry mixed solid components as described in step 1 to start wet mixing. The wet mixing was performed for approximately four minutes.

(4) Casting and vibrating: The fresh mixed GPM or GPC with or without steel fibre was poured into cylindrical plastic moulds of 50 mm in diameter and 100 mm in length, and then vibrated for about one minute to remove air bubbles.

(5) Initial curing and demoulding: After the vibrating and casting, the specimens in the moulds were stored in the laboratory room with a temperature of ~20°C for 24 hours. After the 24-hour initial curing, the specimens were demoulded.

(6) Standard curing: The demoulded specimens were then relocated to a curing room at ambient temperature with a relative humidity of over 90%, where the specimens underwent an additional 28 days of standard curing before they were carried out for the mechanical tests.

2.3 Mechanical tests at elevated temperatures

After they had 28-day standard curing, all specimens were polished on their two end surfaces to ensure the applied loads are to be uniformly distributed on their surfaces during the mechanical test (see Fig. 2). The axial compressive tests at various elevated temperatures were carried out by using the Instron test machine of loading capacity up to 300 kN, that was assembled with an electric furnace which can be heat to temperatures up to 1200°C (see Fig. 3) [24]. Three thermocouples located at different places inside the furnace were used to record the furnace temperature.

During the test of a specimen the electric furnace was first heat to a targeted temperature (20, 100, 300, 500, or 700°C) with the heating rate of 5°C/min. After it reached to the targeted temperature, the furnace was kept with that targeted temperature for another 2 hours to ensure the inside of the specimen had a uniform temperature distribution. After then, mechanical load was applied to the specimen with the rate of 0.002mm/s until the specimen failed. The applied mechanical load was automatically recorded by a computer linked to the Instron machine, whereas the axial deformation and/or axial strain of the specimen being tested was measured and recorded by using the digital image correlation (DIC) equipment mounted in the front of furnace through a rectangular view window on the furnace front, which was also linked to the computer. Note that the deformation or strain measured by DIC does not involve the deformation or strain of the two loading rods and thus they are more reliable and accurate. After the mechanical test was completed an image photo was taken immediately to record the failure mode.

(a) Concrete mixing (b) Concrete casting (c) Concrete curing (d) Surface polishing

Fig. 2 Preparation of GPM and GPC specimens with and without steel fibres

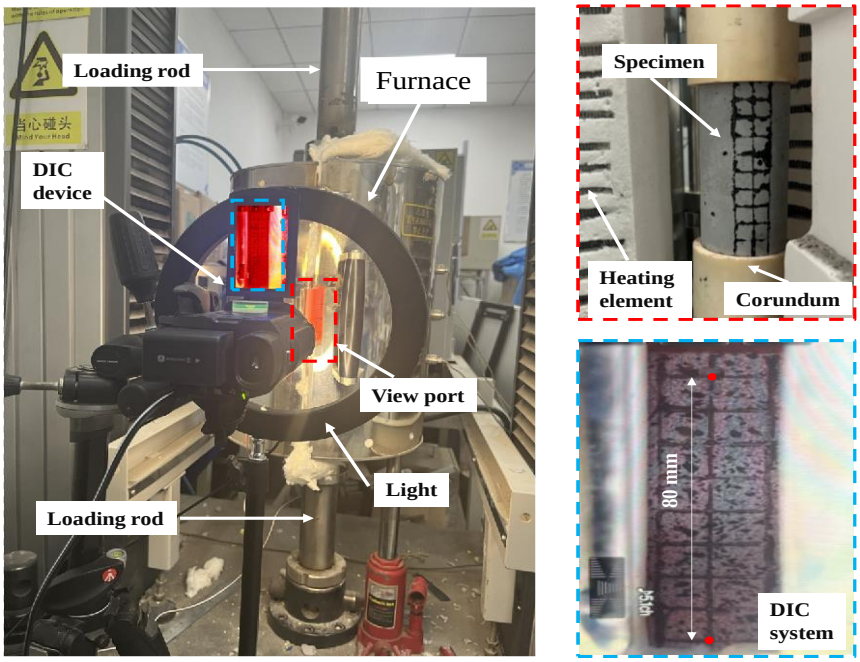

Fig. 3 Instron test machine with an externally assembled electric furnace

3. Experimental results and analysis

3.1 Failure modes

Fig. 4 shows the images of the GPM and GPC specimens with and without steel fibres when they were failed in the axially compressive tests carried out at various elevated temperatures. It can be seen from the figure that the failure modes of the specimens made from GPM and GPC with and without steel fibres are quite different regardless of the temperature. In general, the failure modes of GPM without steel fibres could be characterised by the traditional shear failure; whereas the failure modes of GPC without steel fibres could be considered as the cracking-induced local crush failure where the cracks were initiated at the weaker interfaces between mortar and coarse aggregate. Unlike the specimens without steel fibres, the steel fibre-reinforced GPM and GPC specimens remained integrated when they failed. Their failure modes could be considered as the localised cracking failure. The temperature effect on the failure mode seems not obvious.

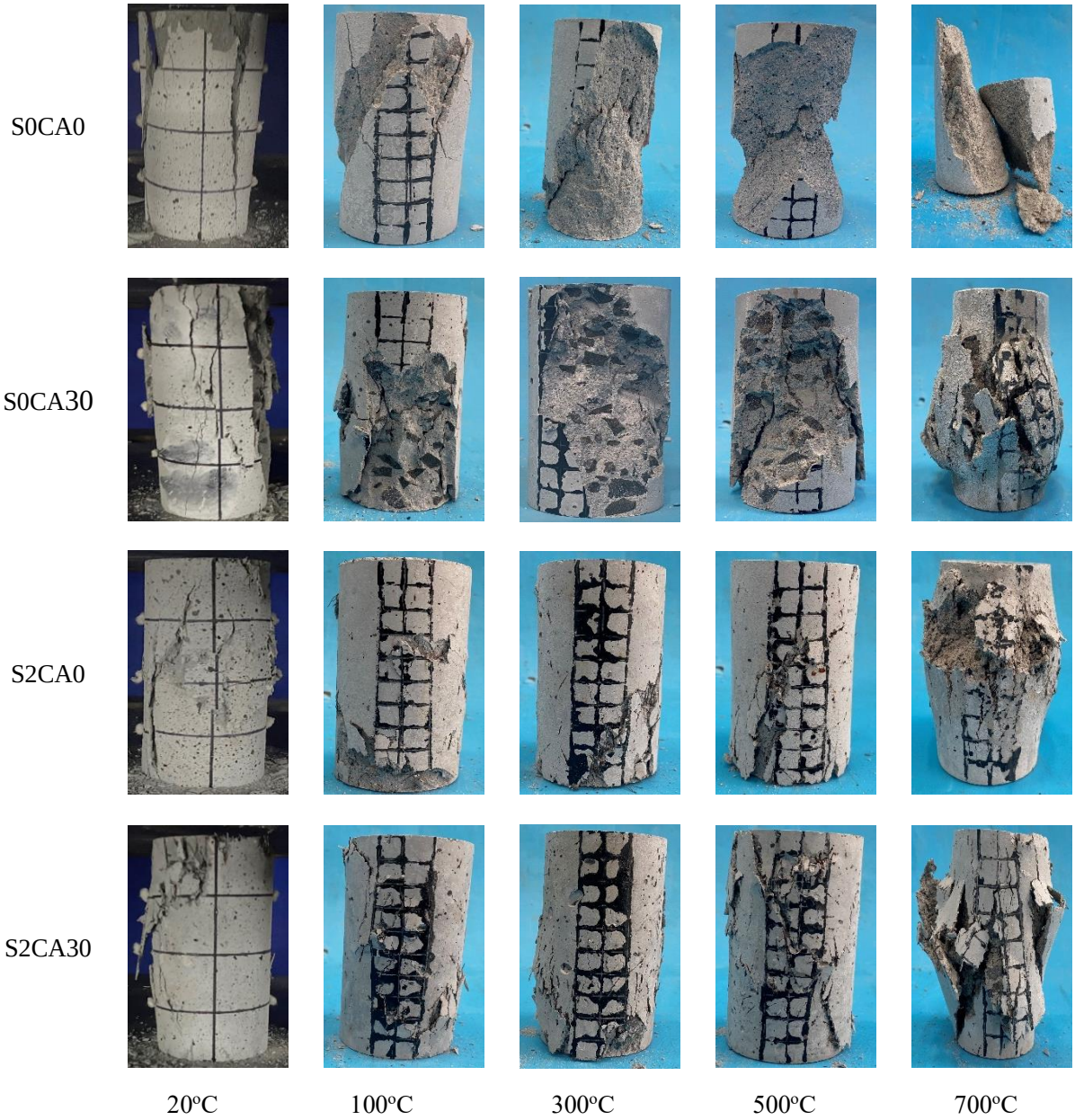

Fig. 4 Failure modes of GPM and GPC specimens with and without steel fibres

3.2 Stress-strain relationship

Fig. 5 shows the stress-strain curves of the GPM and GPC with and without steel fibres obtained from the axially compressive tests carried out at various elevated temperatures. It is well known that, for concrete materials at ambient temperature the stress initially increases linearly with the strain, followed by a nonlinear increase until it reaches to the peak point. After the peak point the stress has a rapid drop with further increased strain. The overall feature of the stress-strain curves of the GPM and GPC at elevated temperatures appears to be similar to that at ambient temperature, except for the stress at the peak point that reduces and the corresponding stain at the peak point that increases with increased temperature. The latter becomes substantial for the high temperature. For the same stress level, the strain in GPC is much smaller than that in the GPM, indicating that the coarse aggregate has an important effect on the deforming ability of GPC. This effect seems to increase with increased temperature. The addition of steel fibres in GPM or in GPC makes a

moderate increase in compressive strength and a large increase in plastic strain. However, this kind of improvement becomes less obvious when the exposed temperature becomes high.

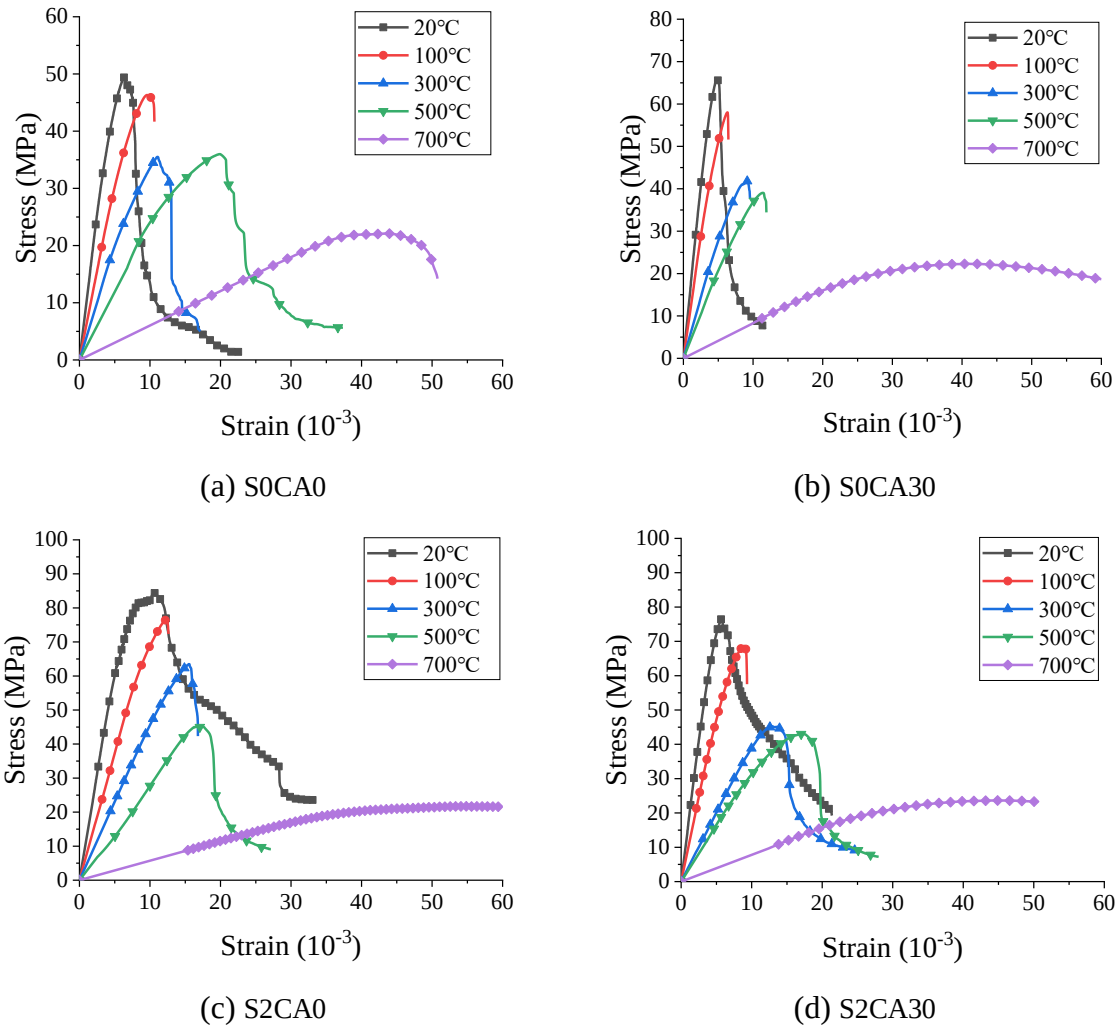

Fig. 5 Stress-strain curves of GPM and GPC specimens with and without steel fibres

3.3 Compressive strength

The compression strength is defined as the maximum stress in the stress-strain curve, that is the stress at the peak point. Fig. 6 shows the compressive strengths of the GPM and GPC specimens with and without steel fibres at different elevated temperatures. It can be seen from the figure that, the GPM reinforced with steel fibres has the highest compressive strength regardless of the exposed temperature, followed by the GPC reinforced with steel fibres. The GPM without steel fibres has the lowest compressive strength. However, in terms of the influence of temperature on the compressive strength, the GPM specimen without steel fibres has the least temperature-induced strength reduction, whereas the GPM specimen reinforced with steel fibres has the greatest temperature-induced strength reduction. The GPC specimens with and without steel fibres have very similar temperature-induced strength reduction, indicating that when both coarse aggregate and steel fibre are present in concrete the coarse aggregate is more sensitive to the temperature.

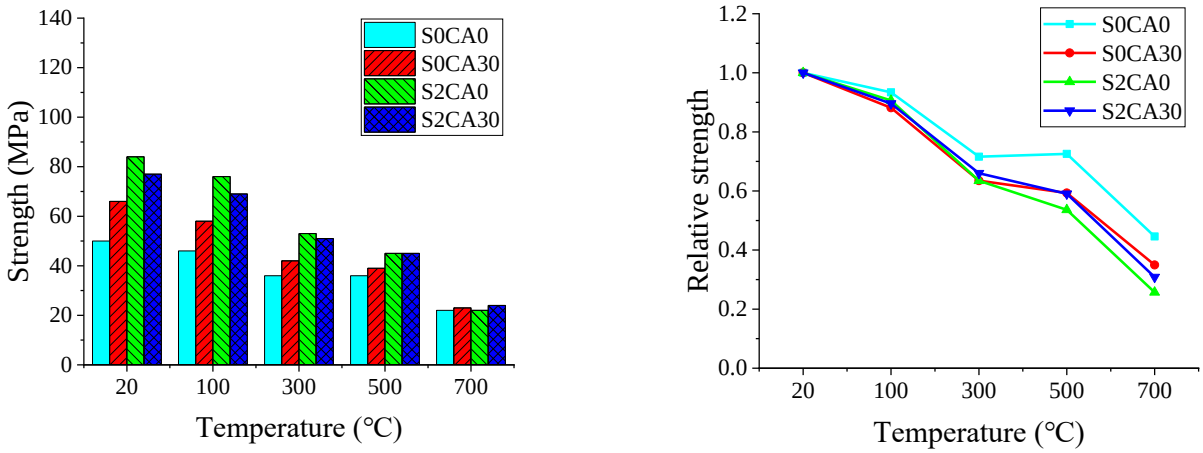

(a) Compressive strength (b) Relative compressive strength

Fig. 6 Compressive strengths of GPM and GPC specimens with and without steel fibres

3.4 Elastic modulus

Fig. 7 shows the elastic modulii of the GPM and GPC specimens with and without steel fibres at different elevated temperatures. In the present study the elastic modulus was determined based on the secant modulus of the stress-strain curve between 0.2 and 0.4 peak stress points. It can be seen from the figure that, up to temperature 500°C the GPC specimen without steel fibres has the highest elastic modulus; whereas the GPM specimen without steel fibres has the lowest elastic modulus, indicating that the steel fibres could improve the stiffness of GPM but not the GPC, particularly when the temperature is not very high. When temperature becomes very high (700°C), there is no big difference in the eleastic modulus between the four tested specimens. Similar to the compressive strength, the elastic modulus also decreases with increased exposure temperature, and the rate of its decrease is generally quicker than that of the compressive strength, which seems to be simila to the OPC concrete [1,24]. Among the four specimens, the GPC reinforced with steel fibres seems to have the quickest elastic modulus reduction, indicating that the temperature has the strongest influence on the elastic modulus of the steel fibre-reinforced GPC than that of the other three mixed concrete.

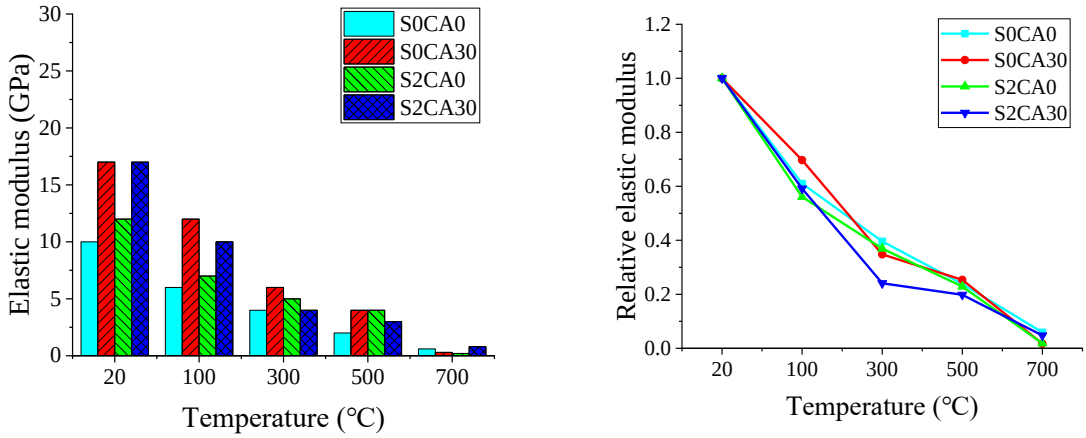

(a) Elastic modulus (b) Relative elastic modulus

Fig. 7 Elastic modulii of GPM and GPC specimens with and without steel fibres

3.5 Peak strain

Peak strain is the stain at the peak point of the stress-strain curve. The peak strain together with the compressive strength and elastic modulus describes the nonlinear behaviour of the ascending part of the stress-strain curve. Fig. 8 shows the peak strains of the GPM and GPC specimens with and without steel fibres at different elevated temperatures. It can be observed from the figure that, for all four tested specimens the peak strain increases with increased temperature. The peak strain of the GPM specimen without steel fibres is larger than that of the GPC specimen without steel fibres regardless of the temperature, indicating that the concrete with coarse aggregate is stiffer than the corresponding mortar regardless the temperature. The use of steel fibres in GPC increases its peak strain in all tested temperature ranges. However, the use of steel fibres in GPM increases its peak strain only when the temperature is not very high (up to 300°C). When the temperature is over 300°C, the peak strains of the GPM specimens with and without steel fibres seem to be very close, indicating that the effect of steel fibres on the peak strain of GPM becomes insignificant when the temperature becomes high.

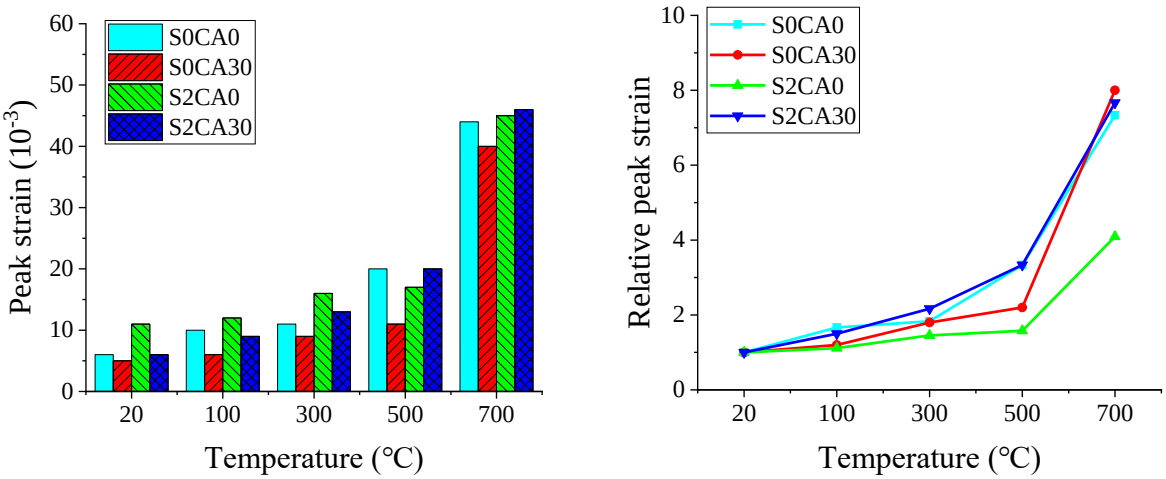

(a) Peak strain (b) Relative peak strain

Fig. 8 Peak strains of GPM and GPC specimens with and without steel fibres

4. Empirical constitutive models of GPM and GPC with and without steel fibres at elevated temperatures

The stress-strain constitutive equations of concrete materials at elevated temperatures are often obtained empirically from experimental data. There are many versions of stress-strain constitutive equations reported in literature [25,26,27]. For example, Li and Purkiss [25] developed a temperature-stress-strain constitutive model for ordinary Portland cement concrete at various elevated temperatures by considering the effect of transient strain. Aslani [27] proposed a compressive stress-strain relationship for both normal- and high-strength GPC at elevated temperatures, which is the modified version of the stress-strain relationship developed by Carreira and Chu [28] for plain concrete at ambient temperature. In either model, the compressive strength, peak strain, elastic modulus, and the slop of descending part of the stress-strain curve are assumed to be temperature dependent and their variation expressions with temperature were obtained empirically from experimental data. According to the experimental data shown in Section 3 for the compressive strength, elastic modulus, and peak strain, we can obtain the following empirical formulas,

$$f_{cT} = f_{c0} \times e^{a_1\left(\frac{T-20}{1000}\right)^{b_1}} \quad (1)$$

$$E_T = E_0 \times e^{a_2\left(\frac{T-20}{1000}\right)^{b_2}} \quad (2)$$

$$\varepsilon_T = \varepsilon_0 \times \left[a_3\left(\frac{T-20}{1000}\right)^2 + b_3\left(\frac{T-20}{1000}\right) + 1\right] \quad (3)$$

where T in ºC is the elevated temperature, f_{cT}, E_T, and ε_T are the compressive strength, elastic modulus, and peak strain at elevated temperature T, f_{co}, E_o, and ε_o are the compressive strength, elastic modulus, and peak strain at ambient temperature, a_1, b_1, a_2, b_2, a_3, and b_3 are the fitting constants used for the compressive strength, elastic modulus, and peak strain, respectively; and their values are given in Table 3 for the GPM and GPC specimens with and without steel fibres, which are obtained from regression analysis. Fig. 9 shows the comparisons of the empirical formulas (1)-(3) and the experimental data, respectively. It can be observed from the figure that there is a good agreement between the proposed empirical formula and the experimental data.

Table 1 Model paramaters used for different mixes

	a_1	b_1	a_2	b_2	a_3	b_3	a_4	a_4	α
S0CA0	-1.1	1.1	-2.7	0.7	11.7	0.012	-1.16	0.02	7.19
S0CA30	-1.4	1	-3.3	0.9	13.6	0.014	-0.58	-0.8	8.89
S2CA0	-2	1.2	-2.8	0.7	6.1	0.006	-0.95	-0.4	2.06
S2CA30	-1.6	1.1	-3.3	0.7	14.3	0.014	-1.13	-0.04	2.13

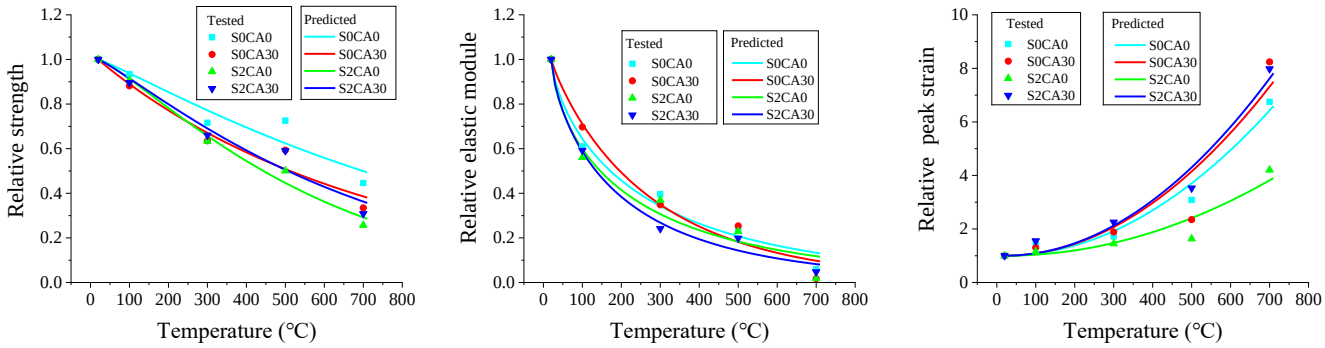

(a) Compressive strength (b) Elastic modulus (c) Peak strain

Fig. 9 Comparisons of empirical formula and experimental data for compressive strength, elastic modulus and peak strain

Similar to our previous work [22,23,29,30,31], the stress-strain constitutive equations of the GPM and GPC with and without steel fibre can be expressed by using two piecewise functions. One is to define the ascending part of the stress-strain curve (x≤1), that is,

$$y = \frac{nx}{(n-1) + x^n} \quad (4)$$

$$n = \frac{E_T \varepsilon_T}{E_T \varepsilon_T - f_{cT}} \tag{5}$$

where $y=\sigma/f_{cT}$ is the dimensionless stress, σ is the compressive stress, $x=\varepsilon/\varepsilon_T$ is the dimensionless strain, and ε is the compressive strain. The other is to describes the descending part of the stress-strain curve ($x>1$), that is,

$$y = \frac{x}{\alpha_T (x-1)^2 + x} \tag{6}$$

$$\alpha_T = \alpha_o \left[a_4 \left(\frac{T-20}{1000} \right)^2 + b_4 \left(\frac{T-20}{1000} \right) + 1 \right] \tag{7}$$

and α_o, a_4, and b_4 are the fitting constants, which are determined according to the experimentally obtained slope of the stress-strain curve and their values are given in Table 3 for the GPM and GPC specimens with and without steel fibres, respectively. To demonstrate the above proposed temperature-dependent stress-strain constitutive equations, Fig. 10 shows the comparisons of the predicted and experimentally obtained stress-strain curves at various elevated temperatures for the GPM and GPC with and without steel fibres. Again, it is evident that there is good agreement between the prediction and test data.

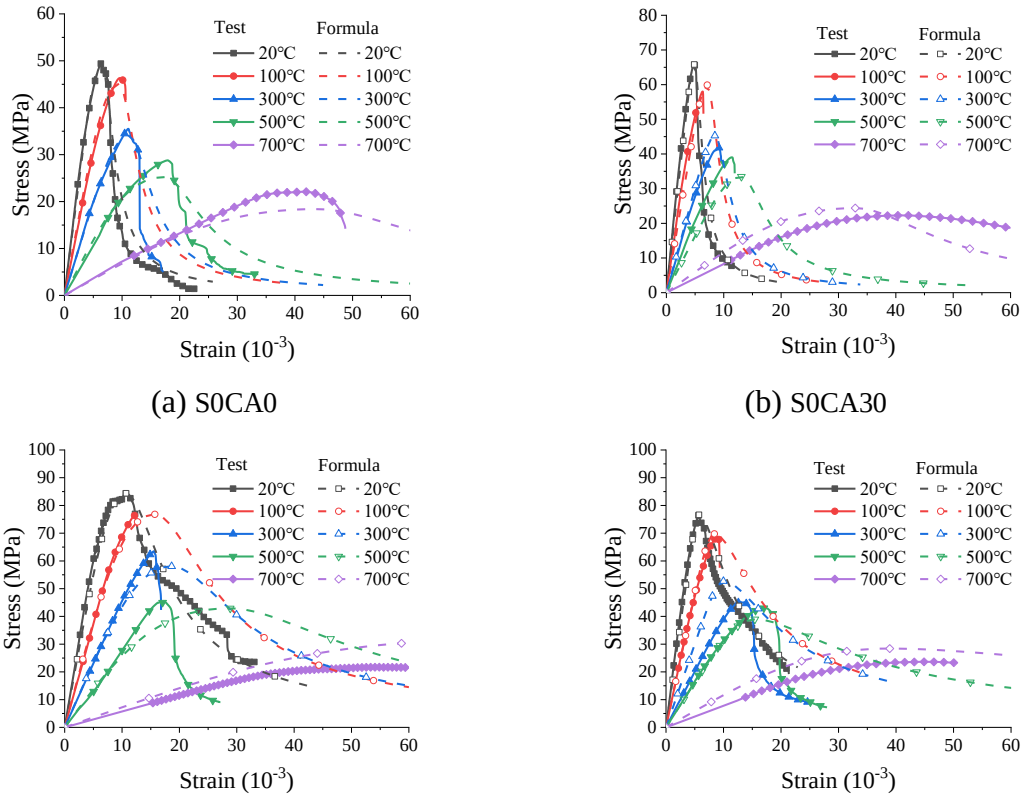

(a) S0CA0 (b) S0CA30

(c) S2CA0 (d) S2CA30

Fig. 10 Comparisons of predicted and experimentally measured stress-strain curves for GPM and GPC with and without steel fibres

5. Conclusions

This paper has presented an experimental investigation on the mechanical behaviour of GPM and

GPC with and without steel fibres when they are exposed to various elevated temperatures. The experimental results on the temperature effects on the compressive strength, elastic modulus, peak strain and ductility of the GPM and GPC with and without steel fibres have been reported. From the present study the following conclusions can be drawn:

- Temperature has a significant influence on the mechanical properties of GPM and GPC with or without steel fibres. The compressive strength and elastic modulus of the GPM and GPC with and without steel fibres decrease with increased temperature, but their peak strain and ductility increase with increased temperature.
- The GPM reinforced with steel fibres has the highest compressive strength regardless of the exposed temperature, followed by the GPC reinforced with steel fibres; whereas the GPM without steel fibres has the lowest compressive strength. The GPC specimens with and without steel fibres have very similar temperature-induced strength reduction.
- Similar to the compressive strength, the elastic modulus of GPM and GPC with and without steel fibres also decreases with increased exposure temperature, and the rate of its decrease is generally quicker than that of the compressive strength. Among the four specimens tested, the GPC reinforced with steel fibres has the quickest elastic modulus reduction, followed by the GPM with and without steel fibres.
- The GPM has larger peak strain than the GPC when they both have no steel fibres regardless of the temperature. The use of steel fibres in GPC increases its peak strain in all tested temperature ranges. However, the use of steel fibres in GPM increases its peak strain only when the temperature is not very high (up to 300°C). For temperature over 300°C, steel fibre has little effect on the peak strain of the GPM specimens.
- The temperature-dependent stress-strain constitutive equation of GPM or GPC with or without steel fibres when exposed to elevated temperatures can generally be characterized by using two piecewise functions. One is for the ascending part of the stress-strain curve which can be defined by the temperature-dependent compressive strength, elastic modulus and peak strain; and the other is for the descending part of the stress-strain curve which can be defined by a temperature-dependent slope of the stress-strain curve.

Acknowledgements - The authors would like to acknowledge the financial supports received from the National Natural Science Foundation of China under grants (No. 52078300 and No. 51978406), the Marie Skłodowska-Curie Individual Fellowships (H2020-MSCA-IF-2020) under grant No. 101022142 (TemGPC), and the Royal Society Joint Project with NSFC, China under grant No. IEC\NSFC\201077.

Declaration of interests - The authors declare that they have no known competing financial interests or personal relationships that could have appeared to influence the work reported in this paper.

References

[1] J.A. Purkiss, L.Y. Li, Fire Safety Engineering, Design of Structures (3rd edition), CRC Press, Oxford (2013).

[2] L.Y. Li, Editorial: Fire safety engineering design of concrete structures, Magazine of Concrete Research 69(7) (2017) 325-326.
[3] Q. Song, M.Z. Guo, T.C. Ling, A review of elevated-temperature properties of alternative binders: Supplementary cementitious materials and alkali-activated materials, Construction and Building Materials 341 (2022) 127894.
[4] W. Tu, M. Zhang, Behaviour of alkali-activated concrete at elevated temperatures: A critical review, Cement and Concrete Composites 138 (2023) 104961.
[5] O.A. Abdulkareem, A.M.M.A. Bakri, H. Kamarudin, I.K. Nizar, A.A. Saif, Effects of elevated temperatures on the thermal behavior and mechanical performance of fly ash geopolymer paste, mortar and lightweight concrete, Construction and Building Materials 50 (2014) 377-387.
[6] H.Y. Zhang, V. Kodur, B. Wu, L. Cao, F. Wang, Thermal behavior and mechanical properties of geopolymer mortar after exposure to elevated temperatures, Construction and Building Materials 109 (2016) 17-24.
[7] H. Su, J. Xu, W. Ren, Mechanical properties of geopolymer concrete exposed to dynamic compression under elevated temperatures, Ceramics International 42(3) (2016) 3888-3898.
[8] F.U.A. Shaikh, A. Hosan, Mechanical properties of steel fibre reinforced geopolymer concretes at elevated temperatures, Construction and Building Materials 114 (2016) 15-28.
[9] X. Jiang, Y. Zhang, R. Xiao, P. Polaczyk, M. Zhang, W. Hu, Y. Bai, B. Huang, A comparative study on geopolymers synthesized by different classes of fly ash after exposure to elevated temperatures, Journal of Cleaner Production 270 (2020) 122500.
[10] X. Jiang, R. Xiao, M. Zhang, W. Hu, Y. Bai, B. Huang, A laboratory investigation of steel to fly ash-based geopolymer paste bonding behavior after exposure to elevated temperatures, Construction and Building Materials 254 (2020) 119267.
[11] H.Y. Zhang, G.H. Qiu, V. Kodur, Z.S. Yuan, Spalling behavior of metakaolin-fly ash based geopolymer concrete under elevated temperature exposure, Cement and Concrete Composites 106 (2020) 103483.
[12] B.A. Tayeh, A.M. Zeyad, I.S. Agwa, M. Amin, Effect of elevated temperatures on mechanical properties of lightweight geopolymer concrete, Case Studies in Construction Materials 15 (2021) e00673.
[13] K. Dhasindrakrishna, K. Pasupathy, S. Ramakrishnan, J. Sanjayan, Rheology and elevated temperature performance of geopolymer foam concrete with varying PVA fibre dosage, Materials Letters 328 (2022) 133122.
[14] M.A. Salih, N. Farzadnia, R. Demirboga, A.A.A. Ali, Effect of elevated temperatures on mechanical and microstructural properties of alkali-activated mortar made up of POFA and GGBS, Construction and Building Materials 328 (2022) 127041.
[15] A. Albidah, A.S. Alqarni, H. Abbas, T. Almusallam, Y. Al-Salloum, Behavior of Metakaolin-Based geopolymer concrete at ambient and elevated temperatures, Construction and Building Materials 317 (2022) 125910.
[16] A.C.C. Trindade, M. Liebscher, I. Curosu, F.A. Silva, V. Mechtcherine, Influence of elevated temperatures on the residual and quasi in-situ flexural strength of strain-hardening geopolymer composites (SHGC) reinforced with PVA and PE fibers, Construction and Building Materials 314 (Part A) (2022) 125649.
[17] S. Xu, M. Zheng, P. Yuan, P. Wu, R. Shao, Z. Liu, J. Liu, C. Wu, Experimental study of mechanical properties of G-UHPC against sodium sulfate attack at elevated temperature, Construction and Building

Materials 396 (2023) 132387.
[18] A.M. Tahwia, M.A. Ellatief, G. Bassioni, A.M. Heniegal, M.A. Elrahman, Influence of high temperature exposure on compressive strength and microstructure of ultra-high performance geopolymer concrete with waste glass and ceramic, Journal of Materials Research and Technology 23 (2023) 5681-5697.
[19] A. Özbayrak, H. Kucukgoncu, H.H. Aslanbay, Y.G. Aslanbay, O. Atas, Comprehensive experimental analysis of the effects of elevated temperatures in geopolymer concretes with variable alkali activator ratios, Journal of Building Engineering 68 (2023) 106108.
[20] K. Liu, J. Liu, J. Li, M. Tao, C. Wu, Experimental investigation of heating–cooling effects on the mechanical properties of geopolymer-based high performance concrete heated to elevated temperatures, Structures 47 (2023) 735-747.
[21] H. Zhang, P.K. Sarker, Q. Wang, B. He, J.C. Kuri, Z. Jiang, Comparison of compressive, flexural, and temperature-induced ductility behaviours of steel-PVA hybrid fibre reinforced OPC and geopolymer concretes after high temperatures exposure, Construction and Building Materials 399 (2023) 132560.
[22] M. Yu, H. Lin, T. Wang, F. Shi, D.W. Li, Y. Chi, L.Y. Li, Experimental and numerical investigation on thermal properties of alkali-activated concrete at elevated temperatures, Journal of Building Engineering 74 (2023) 106924.
[23] M. Yu, T. Wang, Y. Chi, D.W. Li, L.Y. Li, F. Shi, Post-fire micro- and macro-mechanical properties of GGBS-FA-SF blended geopolymer concrete, Construction and Building Materials 411 (2024) 134378.
[24] K. Fan, D.W. Li, N. Damrongwiriyanupap, L.Y. Li, Compressive stress-strain relationship for fly ash concrete under thermal steady state, Cement and Concrete Composites 104 (2019) 103371.
[25] L.Y. Li, J. Purkiss, Stress–strain constitutive equations of concrete material at elevated temperatures, Fire Safety Journal 40(7) (2005) 669-686.
[26] F. Aslani, M. Farhad, Constitutive relationships for normal-and high-strength concrete at elevated temperatures, ACI Materials Journal 108(4) (2011) 355-364.
[27] F. Aslani, Thermal performance modelling of geopolymer concrete, Journal of Materials in Civil Engineering 28(1) (2016) 04015062.
[28] D.J. Carreira, K.H. Chu, Stress-strain relationship for plain concrete in compression, ACI Materials Journal 82(6) (1985) 797-804.
[29] T. Wang, M. Yu, W. Shan, L. Xu, S.S. Cheng, L.Y. Li, Post-fire compressive stress–strain behaviour of steel fibre reinforced recycled aggregate concrete, Composite Structures 309 (2023) 116735.
[30] Y. Yang, L. Huang, L. Xu, M. Yu, H. Ye, Y. Chi, Temperature-dependent compressive stress-strain behaviors of alkali-activated slag-based ultra-high strength concrete, Construction and Building Materials 357 (2022) 129250.
[31] M. Yu, T. Wang, H. Lin, D. Li, L.Y. Li, Experimental investigation of transient strains of GGBS-FA-SF blended geopolymer concrete at elevated temperatures, Construction and Building Materials 419 (2024) 135589.